Journal of Orthopaedic Translation 27 (2021) 25–32

Contents lists available at ScienceDirect

Journal of Orthopaedic Translation

journal homepage: www.journals.elsevier.com/journal-of-orthopaedic-translation

ORIGINAL ARTICLE

De-osteogenic-differentiated mesenchymal stem cells accelerate fracture healing by mir-92b

Yonghui Hou [a,b,1], Weiping Lin [c,1], Ying Li [b], Yuxin Sun [d], Yamei Liu [e], Chen Chen [e], Xiaohua Jiang [f], Gang Li [c,g,**], Liangliang Xu [b,*]

[a] Key Laboratory of Orthopaedics & Traumatology, Guangdong Provincial Hospital of Chinese Medicine, The Second Affiliated Hospital of Guangzhou University of Chinese Medicine, Guangzhou, China
[b] Lingnan Medical Research Center, The First Affiliated Hospital of Guangzhou University of Chinese Medicine, Guangzhou University of Chinese Medicine, Guangzhou, China
[c] Department of Orthopaedics & Traumatology, Faculty of Medicine, The Chinese University of Hong Kong, Prince of Wales Hospital, Shatin, Hong Kong, PR China
[d] Department of Orthopaedics and Traumatology, Bao-An District People's Hospital, Shenzhen, PR China
[e] Departments of Diagnostics of Traditional Chinese Medicine, Guangzhou University of Traditional Chinese Medicine, Guangzhou, Guangdong, 510006, PR China
[f] Epithelial Cell Biology Research Center, School of Biomedical Sciences, Faculty of Medicine, The Chinese University of Hong Kong, Hong Kong SAR, PR China
[g] Stem Cells and Regenerative Medicine Laboratory, Lui Che Woo Institute of Innovative Medicine, Li Ka Shing Institute of Health Sciences, The Chinese University of Hong Kong, Prince of Wales Hospital, Shatin, Hong Kong, PR China

ARTICLE INFO

Keywords:
De-Os-MSCs
Fracture
Mesenchymal stem cells
Mir-92b

ABSTRACT

Background: Mesenchymal stem cells (MSCs) are promising targets for therapeutic use in regenerative medicine and tissue engineering. In the previous study, we have found that MSCs could be reverted to a primitive stem cell population after in vitro induction of osteogenic and de-osteogenic differentiation (de-osteogenic differentiated MSCs, De-Os-MSCs). De-Os-MSCs showed improved cell survival and osteogenic potential. However, the underlying mechanism and its potential effect on fracture healing has not been explored.

Methods: MSCs were isolated from the rat bone marrow. MicroRNAs were cloned into lentiviral vectors and transduced into MSCs to observe the effects on osteogenesis. The expression levels of marker genes were evaluated by quantitative RT-PCR. Ectopic bone formation model was used to evaluate the bone regeneration ability of mir-92b transduced MSCs in vivo. An open femur fracture model was established, and MSCs or De-Os-MSCs were administrated to the fracture sites. Histological, biomechanical and microCT analysis were used to evaluate the quality of bone.

Results: In the present study, we found that mir-92b was significantly increased in the secretions of De-Os-MSCs. And mir-92b could promote the osteogenic differentiation potential of MSCs by activating pERK and JNK signaling pathways. The ectopic bone formation assay showed that MSCs overexpressing mir-92b formed more bone like tissues in vivo. Most importantly, we found local administration of De-Os-MSCs could accelerate fracture healing using an open femur fracture model in rats. The quality of bone property was much better as shown by microCT and biomechanical testing.

Conclusion: Taken together, our study demonstrated that mir-92b promoted osteogenesis of MSCs, which was partially accounted for the enhanced osteogenic differentiation potential of De-Os-MSCs. And De-Os-MSCs had shown better regenerative capacity in accelerating fracture healing when they were locally given.

The translational potential of this article: De-Os-MSCs could be used to accelerate fracture healing, and reduce the occurrence of delayed unions and non-unions.

* Corresponding author. The First Affiliated Hospital of Guangzhou University of Chinese Medicine, Guangzhou University of Chinese Medicine, Guangzhou, China.
** Corresponding author. (Oxon) Room 904, 9/F, Li Ka Shing Institute of Health Institute, Prince of Wales Hospital, The Chinese University of Hong Kong, Shatin, SAR, Hong Kong, PR China.
E-mail addresses: gangli@cuhk.edu.hk (G. Li), xull-2016@gzucm.edu.cn (L. Xu).
[1] Contributed equally as first authors.

https://doi.org/10.1016/j.jot.2020.10.009
Received 29 April 2020; Received in revised form 5 October 2020; Accepted 23 October 2020

Introduction

Fractures are very common large-organ, traumatic injuries in humans [1]. In general, the fracture healing is a complex biological process precisely organized by hormones, cytokines, chemokines, growth factors and other regulators in each stage. Four stages have been found to be involved in fracture healing, including inflammatory response, soft callus formation, hard callus formation and bone remodeling [2]. Although bone has intrinsic regeneration capacity in response to injuries, there are still about 10–20% of fractures result in impaired or delayed healing [3]. Therefore, tissue engineering approach has been developed to favor the regeneration of new functional tissues [4]. And it is extremely necessary to develop therapeutic strategies to accelerate bone regeneration during fracture healing.

Mesenchymal stem cells (MSCs) have been demonstrated as promising targets for therapeutic use in regenerative medicine and tissue engineering, which are characterized by the potential to differentiate into multiple lineages and the ability to be easily expanded ex vivo while retaining their original lineage differentiation commitment [5]. However, the harsh ischemic microenvironment in the fracture sites, infiltrated by the inflammatory and immune cells, provides a significant challenge to the transplanted MSCs. Low cell survival rate and differentiation in vivo are the two main problems hindered the effectiveness of transplanted MSCs [6–9]. Interestingly, it has been found that MSCs are extremely plastic in that they can cross oligo-lineage boundary and trans-differentiate into cells of unrelated lineages, including neurons, hepatocytes and epithelial-like cells under specific conditions [10–13]. Recent studies from both our group and others have demonstrated that dedifferentiation is a prerequisite for MSCs to enhance their capacities [14–17]. However, the underlying molecular mechanisms are largely unknown. Up to now, accumulating evidence has indicated that stem cell fate and function are regulated at the epigenetic level as we learned from pluripotent stem cells [18–20].

It has been well documented that MSCs exert therapeutic effects by differentiating into reparative or replacement cell types, as well as secreting cytokines or chemokines or microRNAs that could potentially repair injured tissues [21–23]. These cytokines/chemokines and RNAs/microRNAs are usually encapsulated in microvesicles or exosomes secreted by MSCs. More than 200 proteins have been identified in the secretion of MSCs, which have the potential to act as paracrine modulators of tissue repair [24]. Our previous study has shown that secretion factors from umbilical cord-derived mesenchymal stem cells can initiate osteogenesis and promote bone repair [25]. Another kind of predominant contents in exosome is microRNAs which play important roles in regulating the functions of MSCs or other cellular processes. For example, mir-126 has been found in stem cell-released exosomes, and mir-126 overexpressed MSCs-derived exosomes could promote angiogenesis in the diabetic rats [26]. It has been revealed that exosomes from MSCs can transfer mir-125b to vascular smooth muscle cells to inhibit the proliferation and migration [27].

Our previous study have shown that after in vitro induction of osteogenic differentiation, MSCs could be reverted to a primitive stem cell population (de-osteogenic differentiated MSCs, De-Os-MSCs) with improved cell survival, colony formation, migratory capacity, as well as osteogenic potential. In the present study, following our previous study, we asked whether De-Os-MSCs could accelerate fracture healing, as well as the underlying mechanism. We found mir-92b was increased in the secretions of De-Os-MSCs. And overexpression of mir-92b in MSCs could promote osteogenesis. Mechanistically, we found mir-92b could activate the pERK and JNK signaling pathways. Finally, we have demonstrated that De-Os-MSCs could accelerate fracture healing when they were directly injected in the fracture sites using the open femur fracture model, which have promising application potential in bone regeneration.

Materials and methods

Culture of rat MSCs

All experiments were approved by the Animal Research Ethics Committee of the authors' institution and carried out in accordance with the approved guidelines. SD rat and GFP transgenic rat were used in the study. Rat bone marrow MSCs were isolated and expanded as previously described [28]. The MSCs were cultured in α-MEM medium supplemented with 10% fetal bovine serum (FBS), 100 U/mL penicillin, 100 mg/mL streptomycin, and 2 mM L-glutamine (all from Invitrogen Corporation, Carlsbad, CA) and cultured at 37 °C, 5% CO_2.

Induction of osteogenic differentiation and de-differentiation

MSCs obtained from the GFP transgenic rat were used. To initiate osteogenic differentiation, MSCs at p3-p8 were transferred to osteogenic induction media (OIM) containing basal media with 1 nM dexamethasone, 50 μM ascorbic acid, and 20 mM β-glycerolphosphate (all from Sigma–Aldrich) for 7–10 days (Os-MSCs). After osteogenic induction, osteogenic media was replaced with basal media and allowed to grow for another 7–10 days (De-Os-MSCs).

Preparation of MSCs secretion and microRNA microarray analysis

The De-Os-MSCs and normal MSCs were cultured in T75 flasks and cultured in α-MEM supplemented with 10% FBS and 1% antibiotics. Then the culture medium was then changed to a plain α-MEM medium that contained no FBS, penicillin/streptomycin, or phenol red. At day 3, 10 mL conditioned serum free medium was collected and filtered with a 0.2 μm filter. Finally, the solution was lyophilized and stored in powder form at −80 °C. For the microarray analysis, 100 μg powder of secretion was dissolved in 1 mL PBS, respectively. The microRNA microarray analysis was performed by the Annoroad Gene Technology Corporation (Beijing, China).

Plasmid construction and lentivirus production

To generate pre-mirs expressing plasmids, the oligonucleotides encoding pre-mir-92b, pre-let-7e, pre-mir-10b, pre-mir-20a, pre-mir-92b, pre-mir-371 and pre-mir-373 were amplified and cloned into the XhoI site of pLL3.7 under the control of U6 promoter. Scrambled control plasmid was also constructed according to the method used by Splinter et al. [29]. Pseudo-lentivirus was produced by transient transfection of 293FT packaging cells (Invitrogen, USA) using the calcium phosphate method. Culture supernatants were harvested at 48 and 72 hour after transfection and lentiviral particles were concentrated using PEG6000 [30]. For transduction, 1×10^5 cells were seeded into 6-well plate and incubated with lentivirus and 8 μg/mL polybrene in the incubator for 24 hour.

Transient transfection

MSCs (1×10^5 cells) were seeded into the wells of a 12-well plate, incubated overnight, and then transfected with miR-92b antagomir (RiBOBIO, China), or negative control using Lipofectamine 3000 (Invitrogen) according to the manufacturer's instructions.

Ectopic bone formation

In vivo studies were performed with the approval of the Animal Experimentation Ethics Committee of The Chinese University of Hong Kong. After anesthesia, an incision was made on the dorsum and a

subcutaneous pocket was created. 2.5 × 10^6 MSCs or mir-92b over-expressing MSCs were seeded onto sterilized Skelite® resorbable Si-TCP bone graft substitute. Then they were transplanted into the same mice. The wound was then closed in layers. At week 8, the scaffolds with cells were harvested and fixed in 10% buffered formalin. Finally, the samples were decalcified, embedded in paraffin and sectioned for histological staining.

Quantitative real time RT-PCR (qRT-PCR)

The cells were harvested and homogenized for RNA extraction with RNeasy mini kit (Qiagen, Hilden, Germany). The mRNA was reverse-transcribed to cDNA by the PrimeScript First Strand cDNA Synthesis Kit (Takara). 5 μl of total cDNA of each sample were amplified in a final volume of 25 μl of reaction mixture containing Platinum SYBR Green, qPCR SuperMix-UDG ready-to-use reaction cocktail and specific primers using the ABI StepOne Plus system (all from Applied Biosystems, CA, USA). The expression of target gene was normalized to that of β-actin gene which was shown to be stable in this study. Relative gene expression was calculated with the $2^{-\triangle CT}$ formula. The sequences of the primers were shown in Supplementary Table 1. To detect the expression of microRNAs, the RNAs were reverse-transcribed to cDNA with the microRNA reverse transcription system (TIANGEN BIOTECH, China). The expression levels of microRNAs were analyzed by qPCR using the miRNAs Quantification Kit (TIANGEN BIOTECH, China). U6 was used as an internal control.

Western blot

Equal proteins were loaded onto 10% Tris/glycine gels for electrophoresis and then transferred to a PVDF membrane (Millipore). Anti-β-catenin (BD, 1:1000), anti-ERK1/2 (BD, 1:2000), anti-phospho-ERK1/2 (BD, 1:1000), anti-phospho-JNK/SAPK (Thr183/Tyr185) (CST, 1:1000), anti-JNK1 (CST, 1:1000) or anti-GAPDH (Santa Cruz, 1:1000) antibodies were used in this study. After washing in TBST, the membrane was incubated with horseradish peroxidase-linked secondary antibodies (anti-mouse or anti-goat) for 1 hour at room temperature. Following TBST washes, protein was detected with the enhanced chemiluminescence blotting reagents (Amersham Biosciences) according to the manufacturer's instruction. The intensity of bands was quantified with Image J software (Image J, National Institutes of Health, USA) and compared statistically.

Fracture healing model and analysis

SD rats were anesthetized with ketamine and xylazine intraperitoneally. The open fracture model was established as previously reported [31]. Briefly, the rats were anaesthetized with ketamine and xylazine. An incision was made over the right femur, then the femur was exposed. The sagittal saw was used to make a mid-femoral transverse osteotomy. An intramedullary 1.2 mm Kirschner wire was inserted to fix the femur. Then the wire was cut and the incision was closed with suture. De-Os-MSCs or normal MSCs were locally injected into fracture sites of SD rat at 7 days after fracture (n = 10). The healing was monitored radiographically using digital x-ray machine. Rats were sacrificed at 3 and 8 weeks after fracture surgery. Femurs were harvested for microCT analysis, and then fixed in 4% buffered formalin, decalcified in 9% formic acid and embedded in paraffin for sectioning. For microCT analysis, the femurs were scanned by vivaCT 40 (Scanco Medical) using our previously established protocols [32]. The scan range covered 3 mm proximal and 3 mm distal to the fracture line with a resolution of 10.5 μm. Low- and high-density mineralized tissues were reconstructed using different thresholds (low attenuation = 160, high attenuation = 350) using our established evaluation protocol with small modification [33]. The high-density tissues represented the newly formed highly mineralized callus and the old cortitces, while the low-density tissues represented the newly formed callus. To assess the mechanical properties of the fractured femur, mechanical test was performed as reported by our department [34]. The sections were subjected to HE or Safranin O staining or immohistochemical staining of OCN as described previously [35]. GFP-labeled MSCs were detected by immunohistochemical analysis using anti-GFP antibody (Santa Cruz).

Histology and immunohistochemistry

Immunohistochemical staining was performed as previously described [36]. The scaffold without and with cells were washed in PBS, fixed in 4% paraformaldehyde, decalcified dehydrated and embedded in paraffin. Sections were cut at a thickness of 5 μm and were stained with H&E after deparaffination. Endogenous peroxidase activity was quenched with 3% hydrogen peroxide for 20 minutes at room temperature. Antigen retrieval was then performed with citrate buffer at 80°C for 10 minutes. Primary antibodies against GFP (1:100; Santa Cruz, CA, USA) and osteocalcin (1:100; Santa Cruz, CA, USA) were used. Donkey anti-goat IgG horseradish peroxidase (HRP)-conjugated secondary antibody and goat anti mouse horseradish peroxidase (HRP)-conjugated secondary antibody (1:200) was then added for an hour, followed by 3, 3' diaminobenzidine tetrahydrochloride (DAKO, Glostrup, Denmark) in the presence of H_2O_2 for signal detection. Afterward, the sections were rinsed, counterstained in hematoxylin, dehydrated with graded ethanol and xylene, and mounted with p-xylene-bis-pyridinium bromide (DPX) permount (Sigma Aldrich, St Louis, MO, USA). Primary antibody was replaced with blocking solution in the negative controls. All incubation times and conditions were strictly controlled. The sections were examined under light microscopy (DMRXA2, Leica Microsystems Wetzlar GmbH, Germany).

Data analysis

Data were presented as mean ± SD. Comparison of two independent groups was done using Mann–Whitney U test. All the data analysis was done using SPSS (version 16.0; SPSS Inc, Chicago, IL). $p < 0.05$ was regarded as statistically significant.

Results

Mir-92b was increased in the secretions of De-Os-MSCs

We have previously reported that after in vitro osteogenic differentiation and de-differentiation, MSCs exhibited enhanced cell survival and osteogenic differentiation potential. As microRNAs have been found to be important regulators of MSCs fate determination, which promoted us to know whether microRNAs are involved in the de-differentiation process. In the present study, the secretions from De-Os-MSCs and normal cultured MSCs were collected for microarray analysis to identify the differentially expressed microRNAs. The top three up/down regulated microRNAs in De-Os-MSCs as found by microarray analysis were listed in Fig. 1A. And the expression levels of these microRNAs were also verified by qPCR analysis (Fig. 1B).

Mir-92b promoted osteogenesis of MSCs

Then we have cloned and overexpressed let-7e, mir-10b, mir-20a, mir-92b, mir-371 and mir-373 in MSCs with lentiviruses. The transfection efficiency was above 80% as confirmed by fluorescence imaging of GFP expression (Supplementary Fig. 1). And the expression level of each microRNA was checked by qPCR analysis (Fig. 1C). The infected MSCs were induced to undergo osteogenic differentiation for 10 days, then the calcium deposits were stained with Alizarin Red S (ARS). The ARS staining and quantification results showed that mir-92b was the most efficient one to promote osteogenesis among the selected six microRNAs (Fig. 1D&E), implying that mir-92b might be one of the main

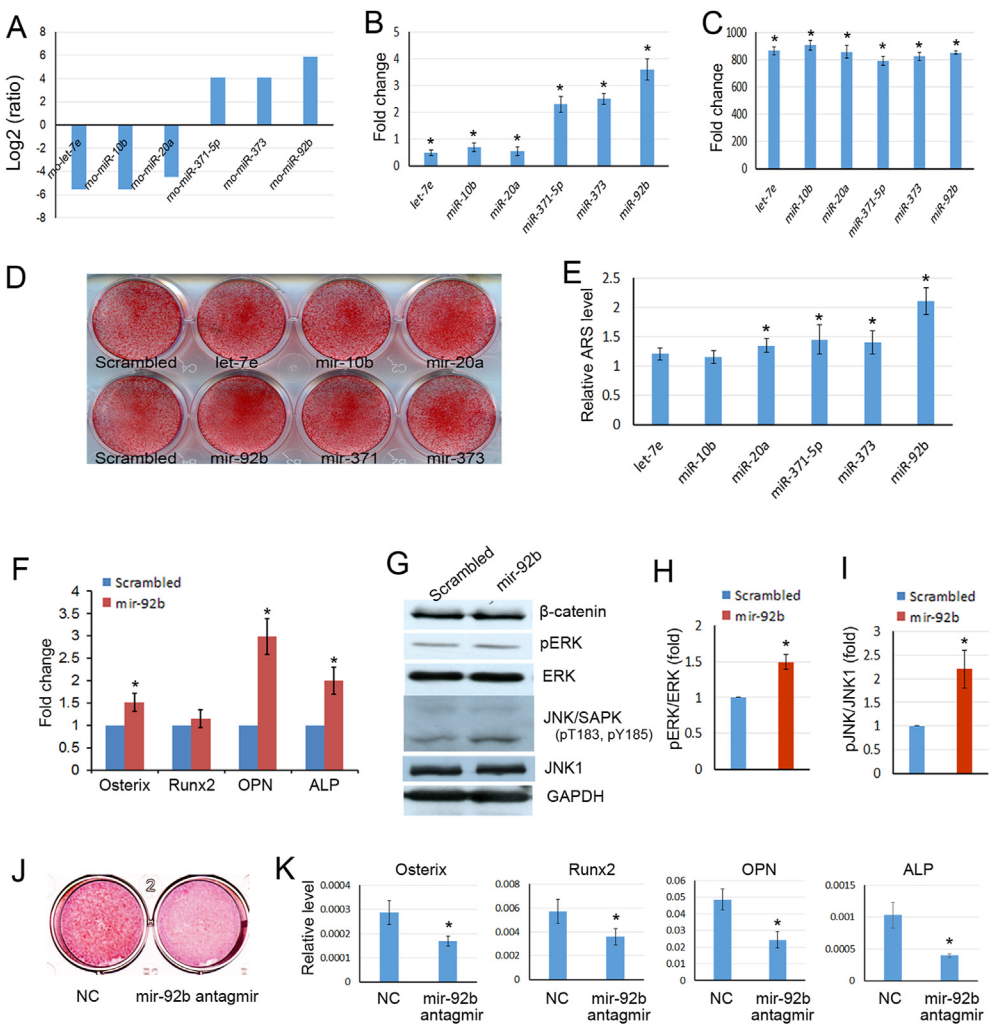

Fig. 1. Mir-92b promoted osteogenesis in MSCs (A–B) The top three up/down-regulated microRNAs in De-Os-MSCs were listed, and verified by qPCR (B) (C–E) The scrambled control, let-7e, mir-10b, mir-20a, mir-92b, mir-371 and mir-373 were transduced into MSCs with lentiviruses. The overexpression of each microRNA was verified by qPCR (C). The infected MSCs were induced to undergo osteogenic differentiation for 10 days, then the calcium deposits were stained with Alizarin Red S (D), and quantified (E) (F) Total RNA was extracted from MSCs infected with mir-92b or scrambled control. The mRNA expression levels of Osterix, Runx2, OPN and ALP were detected by qPCR. β-actin was used as an internal control. The data was expressed as mean ± SD (n = 3). *p < 0.05 (G–I) Total proteins were extracted from MSCs transduced with scrambled control or mir-92b. Then the proteins were analyzed by western blot using indicated antibodies. The protein levels of pERK (H) and pJNK (I) was normalized to ERK and JNK1 respectively. All the data represent mean ± SD of three independent experiments. *p < 0.05 (J–K) The mir-92b antagmir was transfected into MSCs, then the cells were treated with osteogenic induction medium for 10 days, the calcium deposits were stained with Alizarin Red S (J), the changes of osteogenesis-related genes was checked by qPCR (K).

factors leading to increased osteogenic differentiation potential of De-Os-MSCs. We then further evaluated the mRNA expression levels of genes related to osteogenesis by quantitative real time PCR. As shown in Fig. 1F, the expression of ALP (alkaline phosphatase), Osterix and OPN were markedly increased in MSCs overexpressing mir-92b. In addition, we also checked the Wnt and ERK signaling pathways governing the osteogenesis of MSCs. The result showed that the level of β-catenin was not changed by mir-92b, but the levels of phosphorylated ERK and JNK were significantly increased (Fig. 1G–I), meaning that mir-92b might promote osteogenic differentiation by activating ERK and JNK signaling pathways. On the other hand, we also mir-92b antagmir to inhibit the function of mir-92b, and found it could suppress the formation of calcium deposits as well as the expression of osteogenesis-related genes (Fig. J&K). These in vitro results demonstrated that up-regulated mir-92b was accounted for the enhanced osteogenic differentiation potential of De-Os-MSCs.

Mir-92b promoted ectopic bone formation

To further evaluate the promoting effect of mir-92b on osteogenic

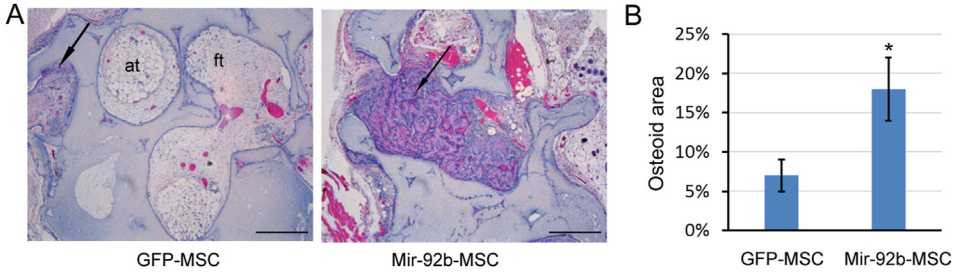

Fig. 2. Overexpression of mir-92b in MSCs promoted ectopic bone formation. MSCs transduced with scrambled/GFP or mir-92b/GFP were loaded onto sterilized porous calcium phosphate restorable granules, and then implanted subcutaneously into the dorsal surfaces. The transplants were harvested 8 weeks later for histological examination (A) The sections were stained with routine hematoxylin and eosin, amorphous osteoid matrix could be seen (arrow head). At: adipose tiusse; ft: fibrous tissue. Scale bar = 400 μm (B) Quantification of osteoid matrix showed that there was more osteoid matrix in mir-92b overexpressing group. Five microscopic fields from each sample were used for measurement. Results are presented as mean ± SD, *p < 0.05.

differentiation of MSCs in vivo, the cells were loaded onto sterilized Si-TCP bone graft substitutes and implanted subcutaneously at the dorsal sides of nude mice. The transplants were harvested 8 weeks later and subjected to histological examination with HE staining to detect the distribution of osteoid. The results showed that MSCs overexpressing mir-92b were superior to GFP transduced MSCs in ectopic bone formation in vivo (Fig. 2).

De-Os-MSCs accelerated fracture healing

Finally, we used open femur fracture model to determine whether De-Os-MSCs could accelerate bone fracture healing. De-Os-MSCs and normal MSCs were locally injected into the fracture sites at 7 days after fracture. At 3 weeks after fracture, the callus from rats that received De-Os-MSCs injection showed larger areas of cartilage as demonstrated by HE and Safranin O staining, indicating that the fracture repair in those rats proceeded through an endochondral ossification process much faster than those in the control groups (Fig. 3A&B). In addition, a larger number of GFP-labeled MSCs were found in the sites of fracture as shown by immunohistochemistry staining (Fig. 3A&C).

At 8 weeks after fracture, the femurs were collected for micro-CT and histological analysis. The newly formed bone (low density bone) in the fracture sites of rats administrated with De-Os-MSCs was higher than the control group, as demonstrated by quantitative data of microCT showing BV_l/TV (Fig. 4A&B), while no differences in BV_t/TV and BV_h/TV (Fig. 4 C&D), suggesting an enhanced bone formation process.

The HE and Safranin O staining as well as immunohistological staining with OCN antibody also showed that more bone formation in the fracture sites of rats transplanted with De-Os-MSCs (Fig. 5A). Through defining the region of interest, we calculated the relative area of bone and cartilage region according to the histological staining. The result showed that only very less cartilage area were seen in the callus of the De-Os-MSCs group (Fig. 5B), while the percentage of bone in callus of rats transplanted with De-Os-MSCs was higher than that of control MSCs group (Fig. 5C).

At last, to confirm functional recovery of the fractured bones, biomechanical evaluation by a four-point bending test was performed. The result showed the percentage ratios of mechanical properties (including ultimate load, energy to failure and stiffness) in the fractured femur vs. the contra-lateral intact femur were significantly higher in the De-Os-MSCs group than that of the control group (Fig. 6A–C).

Discussion

In our previous study, we observed the differences in osteogenesis between MSCs and De-Os-MSCs, and found that epigenetic regulations are probably involved in the dedifferentiation-mediated reprogramming of MSCs. In the present study, we found that mir-92b was responsible for the elevated osteogenic potential of De-Os-MSCs. Most importantly, local administration of De-Os-MSCs in the fracture sites could accelerate bone fracture healing. These results indicated that dedifferentiation could be an important strategy to reinforce the potential therapeutic benefits of MSCs, which could have great impact on the application of MSCs in regenerative medicine.

MicroRNAs are noncoding small RNAs, 21–25 nt in length, encoded in the genome, which can regulate the gene expression by targeting 3' untranslated region (UTR) of mRNAs at posttranscriptional level. Emerging evidence has indicated that miRNAs play important roles in skeletal development and homeostasis [37–39]. The pattern change of miRNAs could be the potential targets for clinical intervention and numerous of studies characterizing miRNAs function in relation to their targets during osteoblast or osteoclast differentiation [40,41]. One of the most studied microRNAs, miR-21, is recognized as a versatile miRNA which involved in lots of biological process, including osteogenesis [42]. Our recent study also demonstrated that mir-21 overexpressing mesenchymal stem cells could accelerate fracture healing in a rat closed femur fracture model [43]. Mir-92b-5p has recently been demonstrated to modulate melatonin-mediated osteogenic differentiation of mouse bone

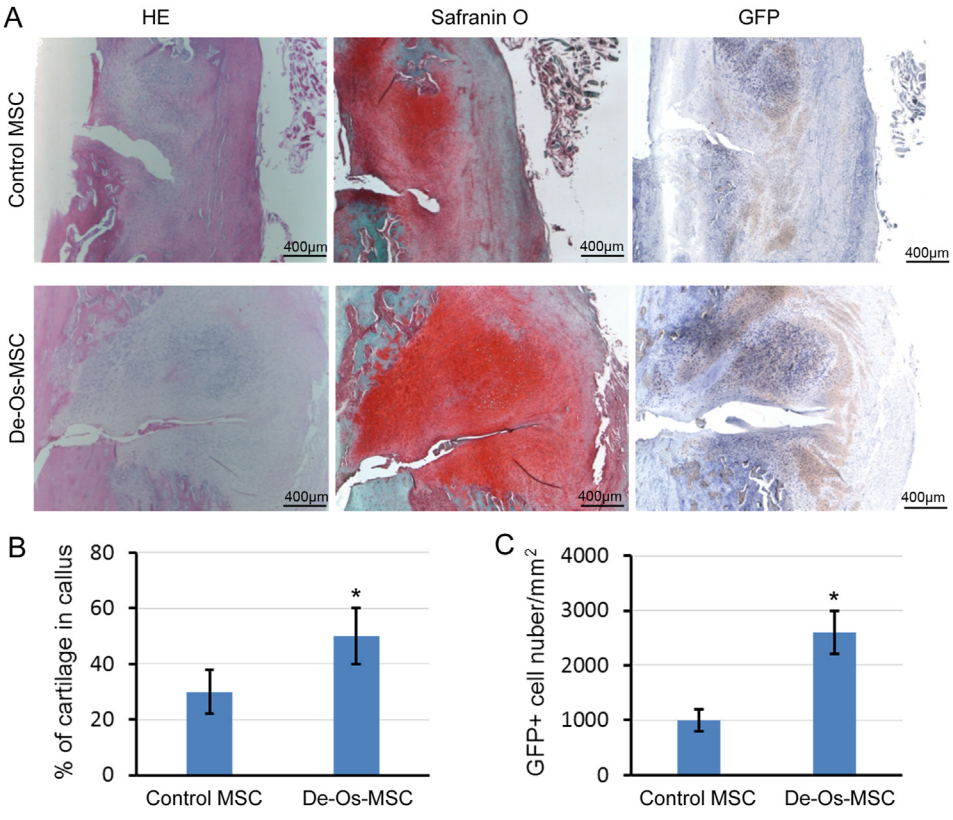

Fig. 3. De-Os-MSCs increased the cartilaginous content in callus at 3 weeks after fracture (A) At 3 weeks after fracture, the femurs were collected for histological analysis. Longitudinal sections of callus were subjected to HE, Safranin O staining and immunohistochemical analysis using GFP antibody (B) The relative cartilaginous area in the callus was measured according to the Safranin O staining (C) The number of locally injected MSCs in callus was counted (n = 3). The data represented mean ± SD. *p < 0.05.

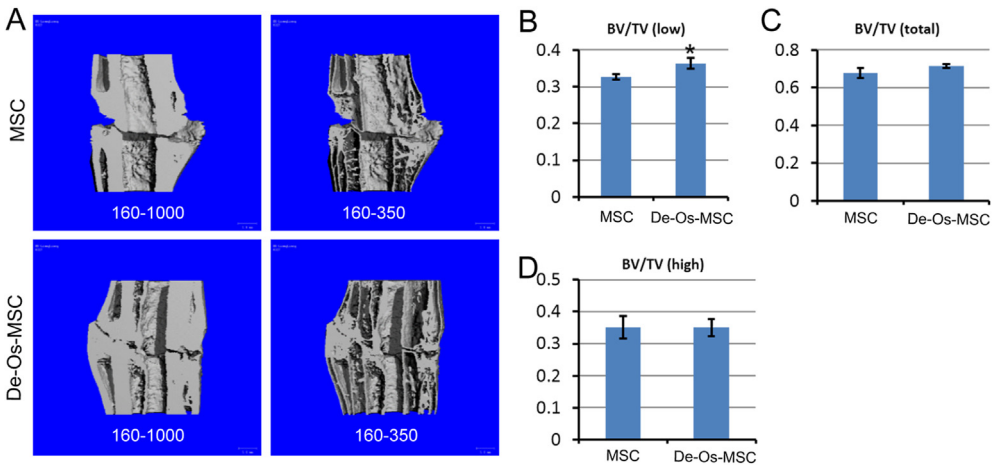

Fig. 4. Micro-CT analysis of fracture callus. At 8 weeks after fracture, the femurs were collected for micro-CT analysis (A) Representative 3D images generated from micro-CT analysis of femur fracture healing in rats transplanted with De-Os-MSCs and normal MSCs (B–D) The bone volume density-BV_t/TV and BV_l/TV was analyzed by micro-CT. TV: Total tissue volume; BV_t: Total bone volume; BV_h: Volume of high-density bone; BV_l: volume of low-density bone. *$p < 0.05$, $n = 4$.

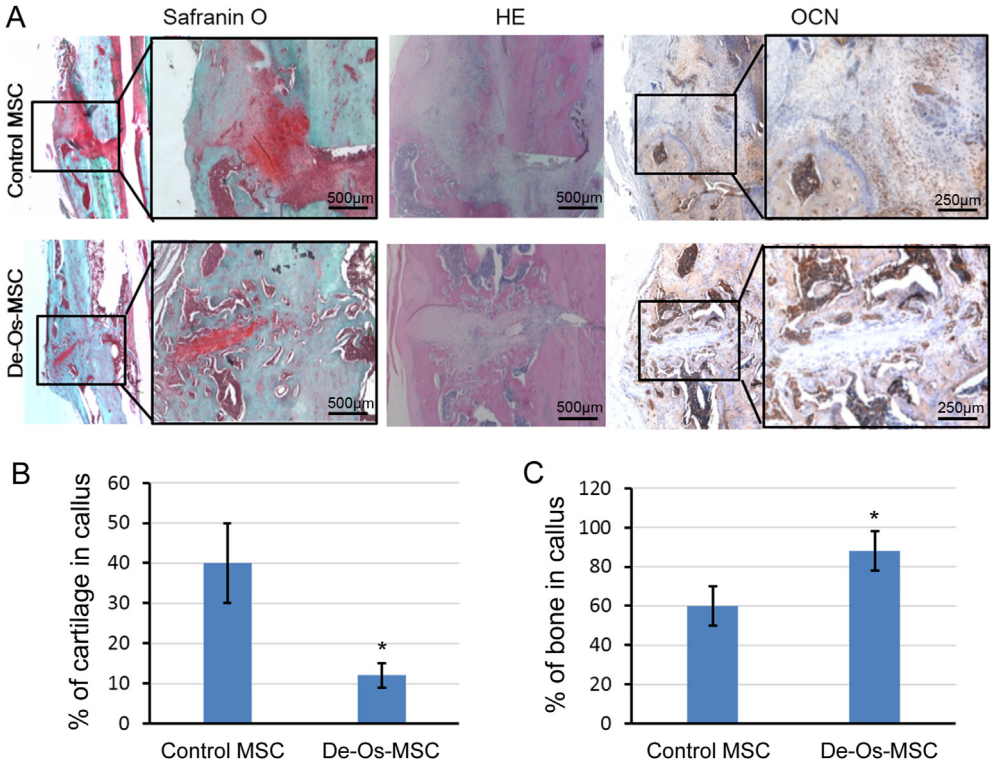

Fig. 5. Histological staining of fracture callus. At 8 weeks after fracture, the femurs were collected for histological analysis (A) Representative images of Safranin O, HE staining and immunohistological staining of OCN in femur fracture callus of rats transplanted with De-Os-MSCs and normal MSCs (B&C) The relative cartilaginous area and newly formed bone in the callus was measured according to the staining. The data represented mean ± SD. *$p < 0.05$.

marrow mesenchymal stem cells by targeting ICAM-1 (intracellular adhesion molecule-1) which is an inhibitor of osteogenesis [44]. Our data is consistent with this finding that mir-92b plays an important role in regulating osteogenesis of bone marrow-derived MSCs. Furthermore, we also found Ezh2 is a potential target of mir-92b by bio-informatics analysis (data not shown). Ezh2 is the catalytic subunit of the Polycomb Repressive Complex 2 (PRC2) and catalyzes tri-methylation of histone H3 at lysine 27 (H3K27me3) to silence target genes. As we have found decreased H3K27me3 and increased promoter accrual of activating histone marks, including H3K4me3 and H4ac on Oct4 gene promoter [17], we believed that down-regulation of Ezh2 mediated by mir-92b might be the underlying mechanism responsible for the changes of histone modifications. However, the bio-informatics analysis also showed many other target genes of mir-92b, we cannot conclude the function of mir-92b is solely mediated by Ezh2. On the other hand, we found pERK and JNK signaling pathways were activated by mir-92b, which could finally lead to the enhanced osteogenesis of MSCs since these pathways are well-known for their function in determining the fate of MSCs [45,46].

Fractures are very common injuries in humans, and about 10–20% of fractures are impaired or delayed during the healing process. So it becomes extremely necessary to develop therapeutic strategies to accelerate bone regeneration during fracture healing. In the present study, we have transplanted De-Os-MSCs to the facture sites to observe whether

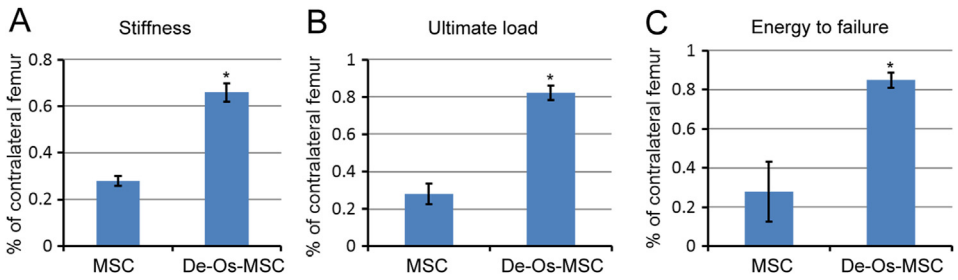

Fig. 6. Mechanical test analysis of fracture callus. At 8 weeks after fracture, the femurs were collected for mechanical test analysis (A–C) Mechanical properties of the fractured bones by four-point bending test. The mechanical properties (including ultimate load, energy to failure and stiffness) in the fractured femur were normalized with contra-lateral intact femur (in percent). The data represented mean ± SD. *$p < 0.05$, $n = 5$.

they could accelerate fracture healing with normal MSCs as control. The results of micro-CT quantitatively exhibited a greater bone volume density in the De-Os-MSCs group compared to that of the control group. The biomechanical evaluation indicated that the percentage ratios of mechanical properties in the fractured femur vs. the contra-lateral intact femur were higher in the De-Os-MSCs group than that of control group. In addition, according to the histological staining, we found that the percentage of bone in callus of rats transplanted with De-Os-MSCs was higher than that of the control MSCs group. These data demonstrated that local administration of De-Os-MSCs could accelerate bone fracture healing. The number of MSCs is an important determinant influencing the effect of MSCs on fracture healing [47], at 3 weeks after fracture we observed that more MSCs were found in the callus in the De-Os-MSCs group.

Taken together, following our previous study showing De-Os-MSCs are superior than normal MSCs in terms of osteogenesis, cell survival and other properties, we have demonstrated that mir-92b was elevated in the secretions of De-Os-MSCs, and mir-92b could regulate osteogenesis by activating ERK and JNK signaling pathways. This finding was consistent with our previous report that epigenetic regulation of Oct4 and Nanog was responsible for the biological differences of De-Os-MSCs. Finally, in an open femur fracture model, we have demonstrated local administration of De-Os-MSCs in the fracture site could accelerate bone fracture healing.

Conclusion

These findings suggest with easy culture manipulation, the dedifferentiation strategy provides a feasible approach to enhance therapeutic efficacy in bone regeneration, which could minimize the occurrence of non-unions.

Data availability statement

The data that supports the findings of this study is available from the corresponding author upon reasonable request.

Conflict of interest

The authors have no conflicts of interest to disclose in relation to this article.

Acknowledgement

The work was partially supported by grants from Guangdong provincial science and technology project (2017A050506046), as well as grants from Hong Kong Government Research Grant Council, General Research Fund (14119115, 14160917, 14120118, 9054014N_CityU102/15 and T13-402/17-N); National Natural Science Foundation of China (81871778); Hong Kong Innovation Technology Commission Funds (PRP/050/19FX and ITS/448/18); and the research was made possible by resources donated by Lui Che Woo Foundation Limited.

Appendix A. Supplementary data

Supplementary data to this article can be found online at https://doi.org/10.1016/j.jot.2020.10.009.

References

[1] Einhorn TA, Gerstenfeld LC. Fracture healing: mechanisms and interventions. Nat Rev Rheumatol 2014;11(1):45–54.
[2] Marsell R, Einhorn TA. The biology of fracture healing. Injury 2011;42(6):551–5.
[3] Axelrad TW, Kakar S, Einhorn TA. New technologies for the enhancement of skeletal repair. Injury 2007;38(Suppl 1):S49–62.
[4] Kon E, Filardo G, Roffi A, Di Martino A, Hamdan M, De Pasqual L, et al. Bone regeneration with mesenchymal stem cells. Clin Cases Miner Bone Metab 2012;9(1):24–7.
[5] Parekkadan B, Milwid JM. Mesenchymal stem cells as therapeutics. Annu Rev Biomed Eng 2010;12:87–117.
[6] Hicks AU, Lappalainen RS, Narkilahti S, Suuronen R, Corbett D, Sivenius J, et al. Transplantation of human embryonic stem cell-derived neural precursor cells and enriched environment after cortical stroke in rats: cell survival and functional recovery. Eur J Neurosci 2009;29(3):562–74.
[7] Li Y, Chen J, Chen XG, Wang L, Gautam SC, Xu YX, et al. Human marrow stromal cell therapy for stroke in rat: neurotrophins and functional recovery. Neurology 2002;59(4):514–23.
[8] Swanger SA, Neuhuber B, Himes BT, Bakshi A, Fischer I. Analysis of allogeneic and syngeneic bone marrow stromal cell graft survival in the spinal cord. Cell Transplant 2005;14(10):775–86.
[9] Chen J, Sanberg PR, Li Y, Wang L, Lu M, Willing AE, et al. Intravenous administration of human umbilical cord blood reduces behavioral deficits after stroke in rats. Stroke 2001;32(11):2682–8.
[10] Jiang Y, Jahagirdar BN, Reinhardt RL, Schwartz RE, Keene CD, Ortiz-Gonzalez XR, et al. Pluripotency of mesenchymal stem cells derived from adult marrow. Nature 2002;418(6893):41–9.
[11] Joshi CV, Enver T. Plasticity revisited. Curr Opin Cell Biol 2002;14(6):749–55.
[12] Petersen BE, Bowen WC, Patrene KD, Mars WM, Sullivan AK, Murase N, et al. Bone marrow as a potential source of hepatic oval cells. Science 1999;284(5417):1168–70.
[13] Woodbury D, Schwarz EJ, Prockop DJ, Black IB. Adult rat and human bone marrow stromal cells differentiate into neurons. J Neurosci Res 2000;61(4):364–70.
[14] Liu Y, Jiang X, Yu MK, Dong J, Zhang X, Tsang LL, et al. Switching from bone marrow-derived neurons to epithelial cells through dedifferentiation and translineage redifferentiation. Cell Biol Int 2010;34(11):1075–83.
[15] Poloni A, Maurizi G, Leoni P, Serrani F, Mancini S, Frontini A, et al. Human dedifferentiated adipocytes show similar properties to bone marrow-derived mesenchymal stem cells. Stem cells 2012;30(5):965–74.
[16] Liu Y, Jiang X, Zhang X, Chen R, Sun T, Fok KL, et al. Dedifferentiation-reprogrammed mesenchymal stem cells with improved therapeutic potential. Stem cells 2011;29(12):2077–89.
[17] Rui Y, Xu L, Chen R, Zhang T, Lin S, Hou Y, et al. Epigenetic memory gained by priming with osteogenic induction medium improves osteogenesis and other properties of mesenchymal stem cells. Sci Rep 2015;5:11056.
[18] Spivakov M, Fisher AG. Epigenetic signatures of stem-cell identity. Nat Rev Genet 2007;8(4):263–71.
[19] Papp B, Plath K. Epigenetics of reprogramming to induced pluripotency. Cell 2013;152(6):1324–43.
[20] Marks H, Stunnenberg HG. Transcription regulation and chromatin structure in the pluripotent ground state. Biochim Biophys Acta 2014;1839(3):129–37.
[21] Schafer R, Northoff H. Cardioprotection and cardiac regeneration by mesenchymal stem cells. Panminerva Med 2008;50(1):31–9.
[22] Chen TS, Lai RC, Lee MM, Choo AB, Lee CN, Lim SK. Mesenchymal stem cell secretes microparticles enriched in pre-microRNAs. Nucleic Acids Res 2010;38(1):215–24.

[23] Liu CH, Hwang SM. Cytokine interactions in mesenchymal stem cells from cord blood. Cytokine 2005;32(6):270–9.
[24] Sze SK, de Kleijn DP, Lai RC, Khia Way Tan E, Zhao H, Yeo KS, et al. Elucidating the secretion proteome of human embryonic stem cell-derived mesenchymal stem cells. Mol Cell Proteomics 2007;6(10):1680–9.
[25] Wang KX, Xu LL, Rui YF, Huang S, Lin SE, Xiong JH, et al. The effects of secretion factors from umbilical cord derived mesenchymal stem cells on osteogenic differentiation of mesenchymal stem cells. PloS One 2015;10(3):e0120593.
[26] Zhu LL, Huang X, Yu W, Chen H, Chen Y, Dai YT. Transplantation of adipose tissue-derived stem cell-derived exosomes ameliorates erectile function in diabetic rats. Andrologia 2018;50(2).
[27] Wang D, Gao B, Yue J, Liu F, Liu Y, Fu W, et al. Exosomes from mesenchymal stem cells expressing miR-125b inhibit neointimal hyperplasia via myosin IE. J Cell Mol Med 2019;23(2):1528–40.
[28] Xu LL, Song C, Ni M, Meng FBA, Xie HQ, Li G. Cellular retinol-binding protein 1 (CRBP-1) regulates osteogenenesis and adipogenesis of mesenchymal stem cells through inhibiting RXR alpha-induced beta-catenin degradation. Int J Biochem Cell Biol 2012;44(4):612–9.
[29] Splinter PL, Masyuk AI, LaRusso NF. Specific inhibition of AQP1 water channels in isolated rat intrahepatic bile duct units by small interfering RNAs. J Biol Chem 2003;278(8):6268–74.
[30] Kutner RH, Zhang XY, Reiser J. Production, concentration and titration of pseudotyped HIV-1-based lentiviral vectors. Nat Protoc 2009;4(4):495–505.
[31] Tagil M, McDonald MM, Morse A, Peacock L, Mikulec K, Amanat N, et al. Intermittent PTH(1-34) does not increase union rates in open rat femoral fractures and exhibits attenuated anabolic effects compared to closed fractures. Bone 2010; 46(3):852–9.
[32] He YX, Liu Z, Pan XH, Tang T, Guo BS, Zheng LZ, et al. Deletion of estrogen receptor beta accelerates early stage of bone healing in a mouse osteotomy model. Osteoporos Int 2012;23(1):377–89.
[33] Hao YJ, Zhang G, Wang YS, Qin L, Hung WY, Kwoksui L, et al. Changes of microstructure and mineralized tissue in the middle and late phase of osteoporotic fracture healing in rats. Bone 2007;41(4):631–8.
[34] Shi HF, Cheung WH, Qin L, Leung AHC, Leung KS. Low-magnitude high-frequency vibration treatment augments fracture healing in ovariectomy-induced osteoporotic bone. Bone 2010;46(5):1299–305.
[35] Tran D, Golick M, Rabinovitz H, Rivlin D, Elgart G, Nordlow B. Hematoxylin and safranin O staining of frozen sections. Dermatol Surg 2000;26(3):197–9.
[36] Rui YF, Lui PP, Lee YW, Chan KM. Higher BMP receptor expression and BMP-2-induced osteogenic differentiation in tendon-derived stem cells compared with bone-marrow-derived mesenchymal stem cells. Int Orthop 2012;36(5):1099–107.
[37] Kobayashi T, Lu J, Cobb BS, Rodda SJ, McMahon AP, Schipani E, et al. Dicer-dependent pathways regulate chondrocyte proliferation and differentiation. Proc Natl Acad Sci U S A 2008;105(6):1949–54.
[38] Gamez B, Rodriguez-Carballo E, Ventura F. MicroRNAs and post-transcriptional regulation of skeletal development. J Mol Endocrinol 2014;52(3):R179–97.
[39] Gordon JA, Montecino MA, Aqeilan RI, Stein JL, Stein GS, Lian JB. Epigenetic pathways regulating bone homeostasis: potential targeting for intervention of skeletal disorders. Curr Osteoporos Rep 2014;12(4):496–506.
[40] Zhang JF, Fu WM, He ML, Xie WD, Lv Q, Wan G, et al. MiRNA-20a promotes osteogenic differentiation of human mesenchymal stem cells by co-regulating BMP signaling. RNA Biol 2011;8(5):829–38.
[41] Zhang JF, Fu WM, He ML, Wang H, Wang WM, Yu SC, et al. MiR-637 maintains the balance between adipocytes and osteoblasts by directly targeting Osterix. Mol Biol Cell 2011;22(21):3955–61.
[42] Bhagat TD, Zhou L, Sokol L, Kessel R, Caceres G, Gundabolu K, et al. miR-21 mediates hematopoietic suppression in MDS by activating TGF-beta signaling. Blood 2013;121(15):2875–81.
[43] Sun Y, Xu L, Huang S, Hou Y, Liu Y, Chan KM, et al. mir-21 overexpressing mesenchymal stem cells accelerate fracture healing in a rat closed femur fracture model. BioMed Res Int 2015;2015:412327.
[44] Li Y, Feng C, Gao M, Jin M, Liu T, Yuan Y, et al. MicroRNA-92b-5p modulates melatonin-mediated osteogenic differentiation of bone marrow mesenchymal stem cells by targeting ICAM-1. J Cell Mol Med 2019;23(9):6140–53.
[45] Kim HY, Park SY, Choung SY. Enhancing effects of myricetin on the osteogenic differentiation of human periodontal ligament stem cells via BMP-2/Smad and ERK/JNK/p38 mitogen-activated protein kinase signaling pathway. Eur J Pharmacol 2018;834:84–91.
[46] Cheng W, Yang S, Liang F, Wang W, Zhou R, Li Y, et al. Low-dose exposure to triclosan disrupted osteogenic differentiation of mouse embryonic stem cells via BMP/ERK/Smad/Runx-2 signalling pathway. Food Chem Toxicol 2019;127:1–10.
[47] Bruder SP, Fink DJ, Caplan AI. Mesenchymal stem-cells in in bone-development, bone repair, and skeletal regeneration therapy. J Cell Biochem 1994;56(3):283–94.